COMPUTER METHODS IN MATERIALS SCIENCE

2021, vol. 21, no. 4, 193–202
https://doi.org/10.7494/cmms.2021.4.0762

Aircraft wing structural design application in MATLAB App Designer

Ahmed Bilal [1]*, Faisal Siddiqui[1], Messam Abbas[1], Mohtashim Mansoor[2]

[1] Department of Aerospace Engineering, Air University A&AC Campus Islamabad, Pakistan.
[2] Department of Aerospace Engineering, College of Aeronautical Engineering, NUST, Risalpur Pakistan.

Abstract

This study focuses on developing an automated application in the MATLAB® App Designer module, based on basic structural members and different theories for various loading cases, providing ballpark values of bending and torsional stiffness and sizing of the load-carrying structural member at a span wise location. All the code developed on MathWorks (2018) is automated using the App Designer module. In this approach, governing equations of structural members under different types of loading are solved in MATLAB IDE with the assumption that in the preliminary phase MATLAB App Designer provides an easy drag and drop type application developer that can be easily subsumed in any mathematical automation process.

Keywords: automated aircraft wing design, aircraft preliminary design phase, wing structure, analytical method, bending and torsional stiffness, MATLAB App Designer

1. Introduction

In the field of aviation, aircraft design has witnessed a great paradigm shift. The automation of the aircraft preliminary design phase has emerged as paramount when designing an aircraft, especially in an era of self-reliance and indigenization. A revolution in software application has produced a Graphical User Interface (GUI) which combines complex ordinary and partial differential equations with a handy input-output based display. This mode has taken the lead in the aircraft design process. The incipient era of design was solely based on the by-hand calculation of the differential equations of the structural members, later supplanted by progress in the computational field and software-based solvers. However, the sequence/phases of design are the same in today's world as those in the past. In the early design phase of aircraft, structural sizing is required to acquire a baseline model. This baseline model for wings includes the structural sizing of load-carrying members and the parameters essential for the selection of wing structural member configuration leading to its selection in subsequent phases, i.e., if a fighter aircraft wing design is under consideration, the final design must subsume the size of load-carrying members, their location, and the number of the load-carrying members to be used. The requirement of automation to acquire a baseline model accentuates the need for analytical solutions that provide a rough estimate of the sizing of structural members and their shape configuration. As in the preliminary design phase, the resources in terms of cost, manpower and computational power are to be minimized, so the use of Finite Element Method (FEM) based solution at this stage is not implemented throughout the aviation industry. This baseline model is used in further aircraft design phases to obtain a more accurate model, so high-fidelity FEM tools are used in the detailed design phase.

* Corresponding author: ahmed.ixloo@gmail.com
ORCID ID: 0000-0002-5502-8559 (A. Bilal)

The workflow in this study can be divided into two areas. The first is the mathematical modelling of a wing for the purpose of design and the second is the use of the MATLAB App Designer module for designing automated software application for this mathematical model. For this study, aircraft structure simplifications, as per the literature, have been implemented while designing the structural design procedure using analytical tools.

1.1. Mathematical modelling of an aircraft wing

1.1.1. External loading

The contribution to the external lift load is due to the pressure distribution on the surface of the wing. This pressure distribution is integrated to form the vertical lift force at the wing's chord wise aerodynamic centre (a.c.), joined together along the span to form a lift line. Secondly, the weight of the wing is used for the inertial loading acting on the wing. It acts at the chord wise centre of gravity (c.g.) location joined together along the span of the wing. Several methods have been devised to calculate the aerodynamic and inertial loading. One such approximate method used in this research is Schrenk's approximation (Bauchau & Craig, 2009) to obtain lift as a function of the wingspan.

1.1.2. Structural dimension

The structure of an aircraft wing is idealized as a box beam (Bauchau & Craig, 2009; Megson, 2017; Dababneh & Kayran, 2014). This wing box is the region occupied by a structural member of the wing, while the leading and trailing edges are reserved for the control surface on the wing. Thus, these areas are practically non-loading carrying regions: structural members which carry the load are not placed in these regions. So the structural web of the wing is further confined in the cross-sectional region.

1.1.3. Structural members

Load-carrying members in the cross-section of the wing are simplified by a specification of the structural member for the defined load type (Niu, 2001, 2002). Further, the sizes of load-carrying members, i.e., spars can be lumped together to form lumped masses and areas (Bauchau & Craig, 2009; Bruhn, 1973; Megson, 2017). These areas are solved for defined loading type, and stress analysis and sizing can be performed.

1.1.4. Loading types

External loading in the aircraft wing cross-section is distributed into different loading types on the structural members, i.e., bending, torsion and shear due to lifting, can be separated and solved separately for stress analysis (Giles, 1971, 1986). The interaction effects of the loading types on each other are assumed to be negligible.

1.1.5. Preliminary sizing

By solving the equation for each loading type for a given cross-section, an initial (rough) idea about the size of the members used in structural design is established. Both the size and location of members can vary and yield a myriad of configurations. However, for the initial design phase that precedes the detailed design phases, rapid and reasonably accurate (approximate 10%) (Niu, 2001) structural dimensions are required. This gives a ballpark figure of the stiffness values required for the loading type (Niu, 2002). It gives a rough idea of the values of stiffness for bending and the torsional load required by the structure.

1.2. Automation of code in MATLAB® App Designer

The automation of MATLAB IDE (MathWorks, 2018) code for wing design was deemed important; the automation of this code (Giles, 1994) will render an interface in the form of a user friendly, easy to use app. For this purpose, the GUI for the said wing design code is modelled using App Designer (MathWorks, 2018); an in-built module in MATLAB 2018. This automation of code can substantially help designers save time in the initial phases of design. The software includes numerous drag-and-drop GUI designing tools, i.e., drop-down tab, radio button, list, tables etc., that can be easily coded for the requirements of the model. A multipage approach is adopted in this process, where each page is designed for a particular subtask of the whole process. This provides a better classification of the different subroutines that are running for that page.

2. Mathematical model

2.1. Lift estimation

In this study, Schrenk's approximation is used: a method formulated for the span wise lift distribution calculation of non-elliptical wings (Raymer, 2018). In this approximation, it is assumed that the load distribution on the wing has a shape that is average lift calculated by both of actual planform and an elliptic shape of the same planform and area as displayed in Figure 1. The area under the lift load curve must sum to the required total lift. Chord of Ellipse is calculated using Equation (1).

$$Ellipse\ chord = \frac{4S}{\pi b}\sqrt{1-\left(\frac{2y}{b}\right)^2} \tag{1}$$

where: S – exposed area of wing planform; b – span; y – element location.

Wing lift is calculated by the formula as shown in Equation (2):

$$Lift(L) = 1.05nW \tag{2}$$

where: n – load factor of the flight; W – maximum take-off weight of aircraft.
As:

$$Lift(L) = qSC_L \tag{3}$$

where: q – the dynamic pressure; C_L – the coefficient of lift.

Lift plotted against the element location, and the lift equation is shown in Figure 2. Lift is the external load due to aerodynamic pressure distribution on the wing's surface thus the lift equation is used in the beam bending equation as an external distributed load to calculate the stress and design parameters of the wing.

2.2. Inertial load

To calculate inertial loading, several approximations need to be made since most of the weight values are not finalized in the preliminary design phase, making approximation a necessity. An approximate method (Raymer, 2018) to calculate wing weight is mentioned. One such method is the use of statistical data to get the value of wing weight.

From Figure 3, the weight per unit area is 44 kg/m^2 for a fighter aircraft wing. This value is multiplied with the planform area of the wing to get the approximate weight. This wing weight is distributed from root to tip based on the area ratio from root to tip, as displayed in Figure 4.

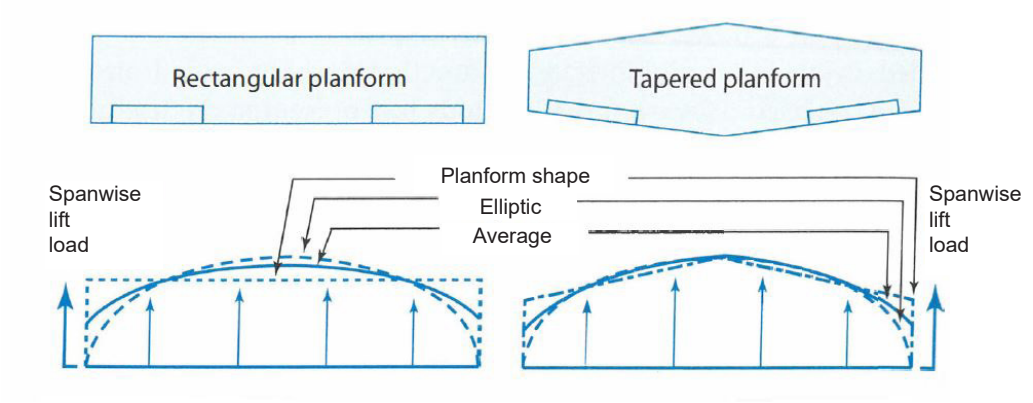

Fig. 1. Aircraft wing lift distribution (Raymer, 2018)

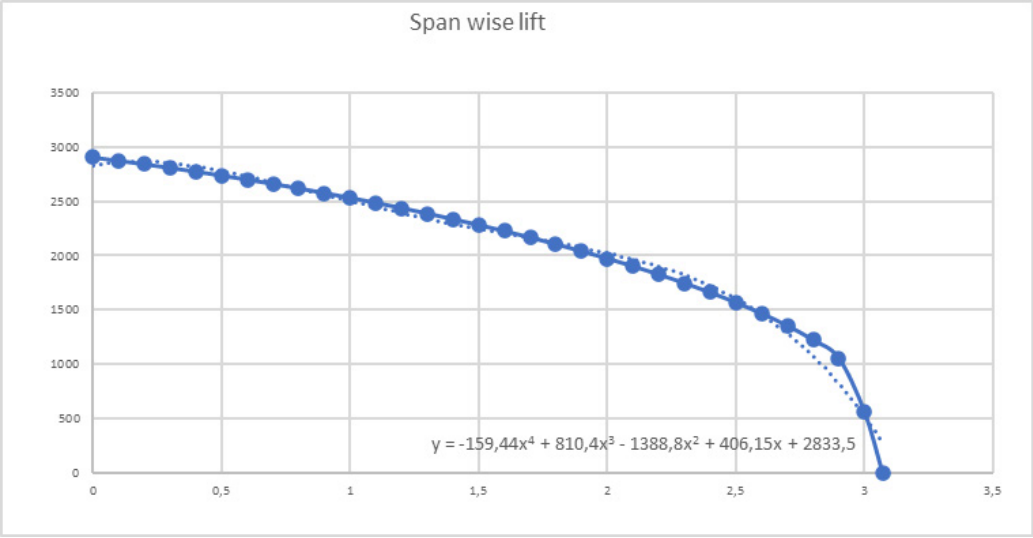

Fig. 2. Lift line equation on wing

	Fighters		Transport & Bomber		General Aviation		Multiplier	Approximate Location
	lb/ft²	kg/m²	lb/ft²	kg/m²	lb/ft²	kg/m²		
Wing	9	44	10	49	2.5	12	$S_{\text{exposed planform}}$	40% MAC
Horizontal tail	4	20	5.5	27	2	10	$S_{\text{exposed planform}}$	40% MAC
Vertical tail	5.3	26	5.5	27	2	10	$S_{\text{exposed planform}}$	40% MAC
Fuselage	4.8	23	5	24	1.4	7	$S_{\text{wetted area}}$	40–50% length
	Weight Ratio		Weight Ratio		Weight Ratio			
Landing gear*	0.033		0.043		0.057		TOGW	centroid
Landing gear—Navy	0.045		—		—		TOGW	centroid
Installed engine	1.3		1.3		1.4		Engine weight	centroid
"All-else empty"	0.17		0.17		0.1		TOGW	40–50% length

Fig. 3. Approximate wing weight chart (Raymer, 2018)

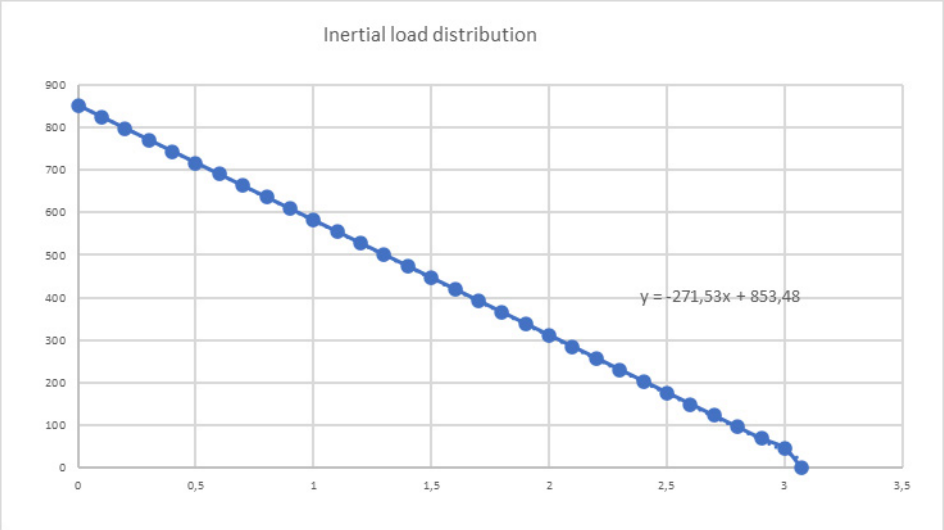

Fig. 4. Inertial load distribution along span

2.3. Wing box beam model

The box beam design (Bauchau & Craig, 2009; Dababneh & Kayran, 2014) of the wing is an extension of the simple cross-section structure as in Figure 5 and 6, solved for bending, torsion and shear loading. In this study, the basic model is selected as this model provides a good enough estimate of structural load carrying members' size (Niu, 2001, 2002).

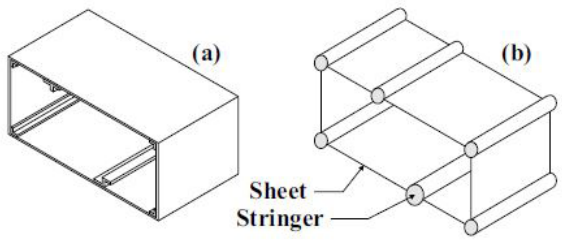

Fig. 5. Wing structure idealization (Bauchau, 2018)

In the box beam, some variables are selected based on which the wing spar and skin thickness optimized solution can be obtained.

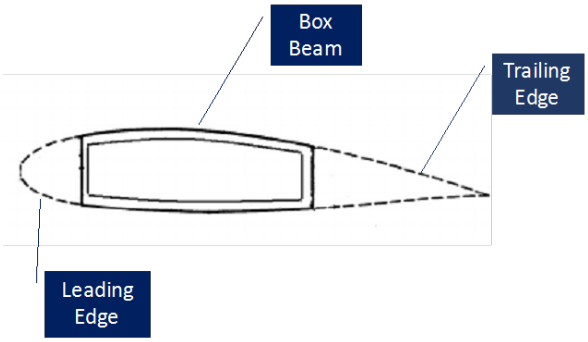

Fig. 6. Wing box beam (Megson, 2017)

Design variables in the problem formulation in this study are as below. These are the input variables (Dababneh & Kayran, 2014) for study from which we can formulate and observe changes in the dependent objective function:

- structural design variable:
  - skin thickness,
  - lumped area of flanges,
  - location of spars,
  - wing orientation,
  - ribs thickness at bay location;

– geometric design variables:
  • aerodynamic centre location,
  • center of gravity location;
– material variables:
  • yield stress,
  • modulus of elasticity;
– design factors:
  • factor of safety (FoS),
  • load factor (n).

2.4. Internal loading formulation

For loading and stress analysis, 10 equidistant span wise bays are selected (Oden, 2014). At these bay locations, cross-section geometric properties are calculated, and for this value the equation of beam bending, torsion and shear loading is solved. The values of spar flange area and skin thickness are calculated at these bays. Thus, these values can be interpolated in between the bays. Calculation for stiffness, bending moment, shear force, lump area and skin thickness are done at bay locations. Euler–Bernoulli beam equation is used to solve the beam bending. The governing differential equation of a beam under bending load is given in Equation (4) (Bauchau & Craig, 2009). Figure 7 shows the axis system used in the code along with the generic load types with their abbreviations.

$$\frac{d^2}{dx_1^2}\left(H_{22}\frac{du_3^2}{dx_1^2}\right) = p_3 + \frac{d}{dx_1}(x_3 \cdot p_1 + q_2) \tag{4}$$

where: H_{22} – the bending stiffness; u_3 – the transverse displacement; x_3 – the offset of axial distributed load from the centroidal axis.

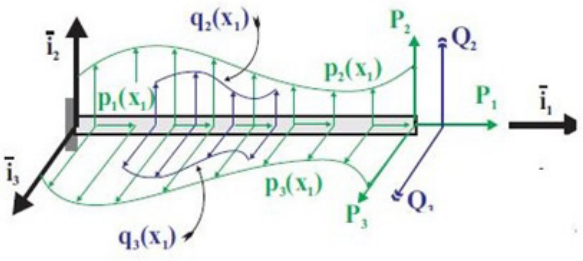

Loading Type	Notation	Units
Distributed loads	$p_1(x_1), p_2(x_1), p_3(x_1)$	N/m
Concentrated loads	$P_1^{[k]}, P_2^{[k]}, P_3^{[k]}$	N
Distributed moments	$q_2(x_1), q_3(x_1)$	N.m/m
Concentrated moments	$Q_2^{[k]}, Q_3^{[k]}$	N.m

Fig. 7. Euler–Bernoulli beam bending (Bauchau, 2018)

In this study, the beam is acted upon by distributed lift load and inertial load along the i_1 direction (span wise direction). The equation of the loading is calculated as:

Inertial distributed load: $(-271.53x_1 + 853.48) \cdot S$
Aerodynamic distributed load:
$(-159.44x_1^4 + 810.4x_1^3 - 1388.8x_1^2 + 406.15x_1 + 2833.5) \cdot S$

In the general beam equation, these two loadings are inserted in Equation (4) as p_3. For beam, axial stress arises due to bending load is given by Equation (5):

$$\sigma_1^r = E^r\left[\frac{N_1}{S} + x_3^r\frac{H_{33}M_2 + H_{23}M_3}{\Delta H} - x_2^r\frac{H_{23}M_2 + H_{22}M_3}{\Delta H}\right] \tag{5}$$

where: E^r – the young modulus of the respective boom under consideration, x^r, y^r – its coordinates; H_{23}, H_{33}, H_{22} – the cross bending and bending stiffness of the box beam at the bay location. ΔH is equal to $(H_{22} \cdot H_{33} - H_{23}^2)$.

Shear load in wing cross-section is due to the lift and inertial loading. In the case of the thin-walled beam, as the wing is modelled as a thin-walled beam, stress flow is a parameter used to gauge the value of shear stress in beam sheets. As the assumption was made previously, that skin will not be carrying the axial load, so this thin skin section shear stress within two booms is constant, as shown in Figure 8:

$$\frac{\partial n}{\partial x_1} + \frac{\partial f}{\partial s} = 0 \tag{6}$$

where: n – axial stress flow; f – shear flow; x_1, s – the axial and curvilinear sheet direction coordinates.

Equation (6) shows that in the absence of any axial stress flow in sheets (Megson, 2017) Equation (6) reduces to:

$$\frac{\partial f}{\partial s} = 0 \tag{7}$$

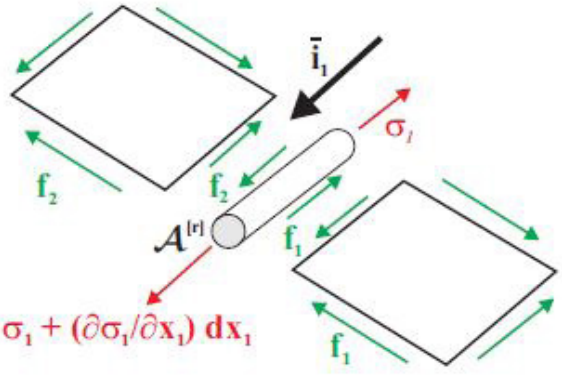

Fig. 8. Stringer sheet idealization of wing structure (Bauchau, 2018)

$$\Delta f^r = -E^r A^r \left[x_2^r \frac{H_{22}V_2 - H_{23}V_3}{\Delta H} - x_3^r \frac{H_{23}V_2 - H_{33}V_3}{\Delta H} \right] \quad (8)$$

where the V_2 and V_3 are the shear forces in i_2 and i_3 directions respectively.

The method of cut (Bauchau & Craig, 2009; Megson, 2017) is used to calculate the shear flow in the beam box. It is pertinent to mention here that the code designed to solve this part caters for the change in a number of cells as we move to span wise due to restricted length of spar by the slope of wing owing to sweep of leading and trailing edges. The beam solution in this study assumes a uniform torsion case which assumes that the rate of twist κ remains constant in the axial direction. Bredt–Batho equation derived for the solution of the torsion problem for this walled structure will be used. The Equation (9) is given as below:

$$M_1 = \sum_i^n 2A_i f_i \quad (9)$$

where: A – the area enclosed by the cell; n – the total number of cells at the wing cross-section.

The second equation used is by the assumption of uniform torsion. This shows that the rate of twist in each cell at a particular cross-section is equal, so by using the rate of twist of each cell, the number of equations can be made equal to the number of unknowns; here, the unknowns are f in each cell.

$$\kappa_1 = \kappa_2 = \kappa_3 \ldots \ \ldots = \kappa_n \quad (10)$$

$$\kappa_i = \frac{1}{2A_i} \int_c^i \frac{f^i}{Gt} ds \quad (11)$$

where G is the shear modulus of the skin material, and integral represents closed integral for each cell with respect to the curvilinear coordinates.

For the ribs sizing, its location is selected as the location of bays. Ribs are assumed as a sheet of uniform thickness placed at the bay location. Its sizing is done based on shear flows calculated as mentioned. The scheme followed in this study is first to consider a single spar wing with lumped areas and calculate the value of axial stress in it. Equate the beam stress in boom to the yield stress limit with incorporated FoS will yield the single spar lumped area required. This value can be divided into multi-spar cases for optimal configuration design. The areas of booms acquired through these code runs are inserted into the actual beam model code, and then a solution of shear flow in the skin is carried out with the values calculated in the previous two runs. The iterative process to compare the value of shear stress in a sheet with the shear stress limit value converges to provide the skin thickness required to carry the internal load by the skins. Thus, the resultant function (weight of the wing structure) is calculated based on the interpolation of skin and spar area values at bay locations.

3. Automation of wing design code

MATLAB App Designer module is used for the automation and interfacing code for users (Youhua, 2000; Youxu et al., 2012). The GUI (Fig. 9) and mentioned module provides independence for the user in selecting various drag and drop tools for, e.g, input (Fig. 10) and output data. Displaying the data is also integrated into the software so that an easy and effective demonstration of data can be carried out on the interface page. The tools are present in the component library toolbox (Fig. 11), with several sub tools grouped together. Each tool is designed on a drag and drop theme with it can be displayed on the interface page. The interface page contains two views: *Design* and *Code* views. These view pages can be selected by a button on the design page. At the code view page (Fig. 12), each tool needs to be coded for the type and nature of data to be carried in the code. The syntax of code is simple, and wing design parameters are mapped on these tools. On the design page, the display parameters of the tools and tables can be altered as required by the user on the actual display page. Once the format of the page and the tools definition in the GUI are carried out, the page can be tested using a run button, and the page will be displayed as per the settings defined in the designing phase.

Automation for wing design is carried out on a multi-paged GUI theme. *Front Page* of the app is designed to access other pages of app based on the functionality of each page. All the pages are in actual fact independent apps that are being accessed through the call back button tab functionality in App Designer module. The sequence is to first access *Variable Inputs* page from the drop-down menu on front page to insert the material and geometric inputs as shown in Figure 12 and 13. Once the inputs are defined, the initial calculation for one spar case is to be accessed by *Boom Area* page selection. Afterwards, the design of the selected spar as per the user design is accessed. The sectional properties, stress check, displacement and rotation mentioned are calculated and displayed in the form of tables, figures, and prompt boxes.

3.1. Front page GUI

Front page of GUI design, shown in Figure 9, uses two library components from App Designer; drop down menu box which displays the list of all apps pages that can be accessed from it and a callback button. Any apps from this menu can be selected by clicking on drop down menu and selecting the required app. The next step is to click the *Go* button on the page. This button is used as a call-back function initiator for calling the app as per the selection of the user.

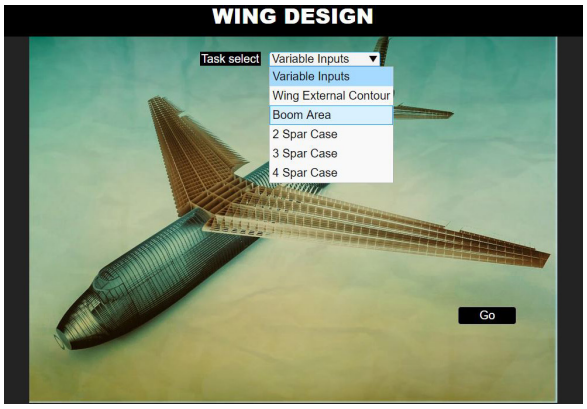

Fig. 9. *Front Page* with drop-down menu

3.2. Variable input GUI

The first tab in the drop-down menu is that of *Variables Input*. This page is used to define the geometric and material variables as per the user requirement. The display page of variable input GUI is shown in Figure 10. The list of the variables defined on this page are divided into two types:

- geometric variables:
  - sweep angle leading edge,
  - sweep angle trailing edge,
  - length,
  - length of chord at wing root;
- material variables:
  - young modulus skin,
  - young modulus spar,
  - yield stress spar,
  - yield stress skin,
  - shear strength skin,
  - shear strength spar,
  - shear modulus spar,
  - shear modulus skin,
  - density skin,
  - density spar.

These input values are defined as global and can be imported into other pages of GUI. Once the values are inserted, *Button* is to be pressed to have variables defined as global.

3.3. Wing external contour GUI

The external contour of the wing is drawn on this page (Fig. 11). External contour geometric parameters are imported on this page via the *Import* button. The selection of spar for display is made via the radio button *Selection* pane.

Once the spar is selected, the location of the spar is placed in, and *Go* button is pressed to run the code. This will display the wing contour in the form of a figure.

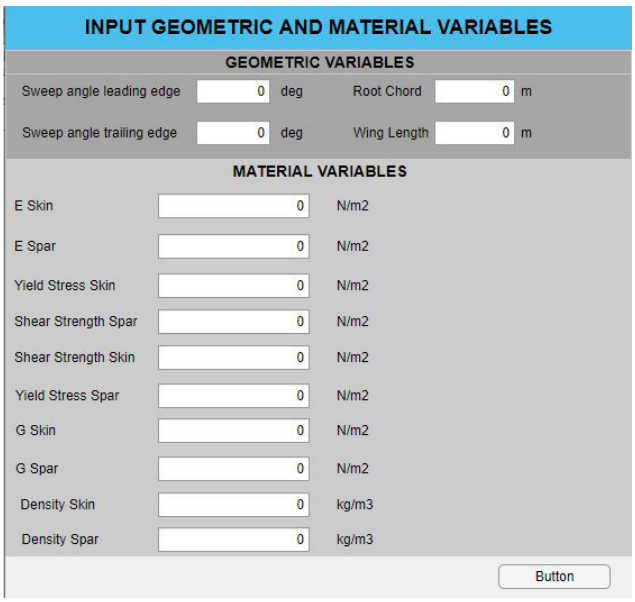

Fig. 10. Variable input page

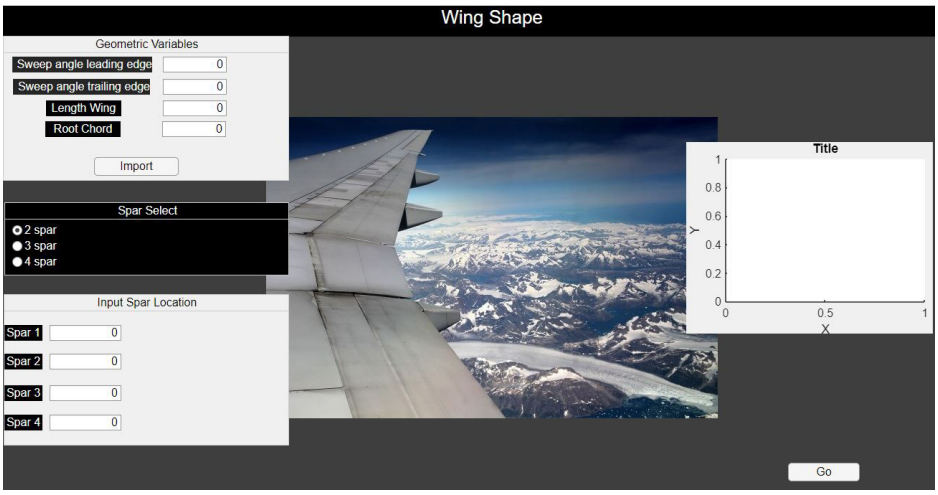

Fig. 11. External contour page

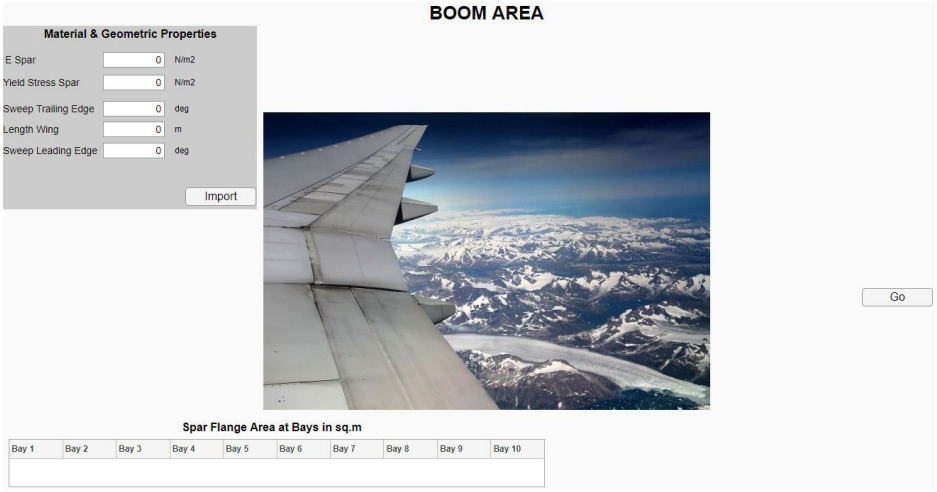

Fig. 12. *Boom Area* page

3.4. Boom area GUI

This page is used to calculate the initial size of spar according to the material properties selected by the user in the previous page. The values of the boom flange area (symmetric) are displayed on the page in the form of a list, as shown in Figure 12. The predefined geometric and material properties are imported on this interface using the *Import* button. Once the properties are imported, the *Here we go* button is used to run the code. After the code run is completed, the table on the bottom right labelled *Spar Flange Area* at *Bays in sq m* displays the values of the area at bays.

3.5. 2, 3 & 4 spar wing design GUI

This page is designed for the analysis and display of the main sectional properties of wing design at specified bay locations (Fig. 13). These properties include:

- *Wing Shape* with spars, centroidal axis and elastic axis;
- *Bending* and *Torsional Stiffness* along span;
- *Weight of Spar, Skin and Ribs*, *Total Weight*;
- Deflection and rotation of wing at any point.

The interface is designed to import previously defined variables using the *Import* button, and spar location is defined in the *Input Variables Panel Box*. The value of displacement and rotation at any span wise location and displacement at any point on the wing is also calculated. Span wise lateral and transverse points are defined by the user and values for displacement and rotation is displayed in the *Output Displacement / Rotation Panel Box*. At the right lower bottom of the page, the axial stress ratio is displayed. This is the ratio of actual stress at bay to the allowable limit of stress as per the material and FoS specification.

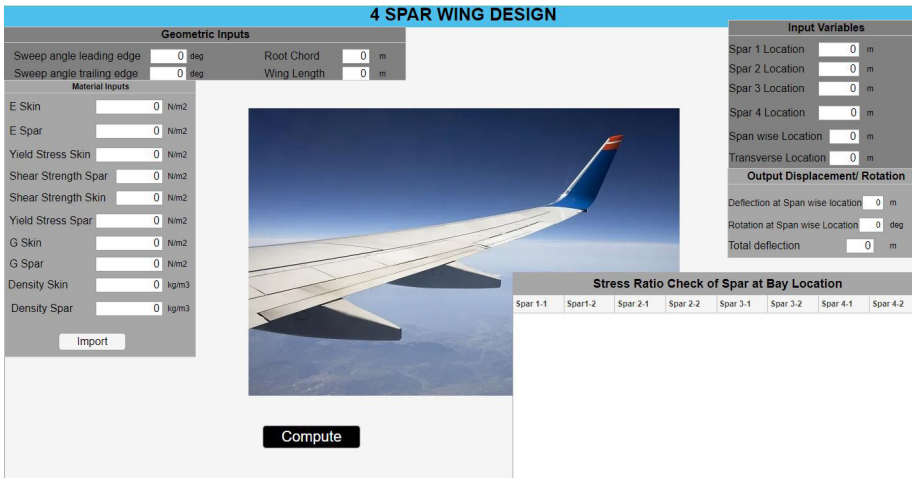

Fig. 13. *4 Spar Wing Design* page

4. Results and validity check

The stress ratio check panel box is 1 or −1; this means the spar stresses are within the limited stress value at each bay location (Fig. 14). This is one of the check points for code validity.

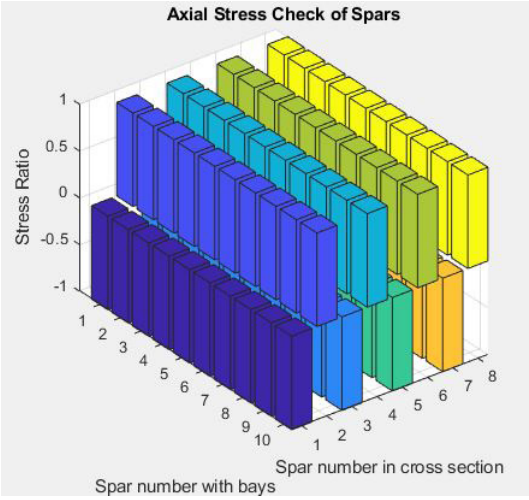

Fig. 14. Axial stress ratio

Wing top view with the spar location, the centroidal axis of the wing and elastic axis of the wing is displayed as shown in Figure 15. This is in line with the expected result as both elastic and centroidal axes are geometric properties and must be at the centre if the cross-section is symmetric. This is our second check point for the validity of the code.

Wing weight is one of the objective functions on which the optimal configuration is determined. The weight of spar, skin and total weight is displayed as shown in Figure 16. Weight calculation is done by linearly interpolating the value of spar area and skin thickness at bay locations and calculating the volume of the structure. This volume is subsequently multiplied by the density of the designated material of spar and skin to get the weight.

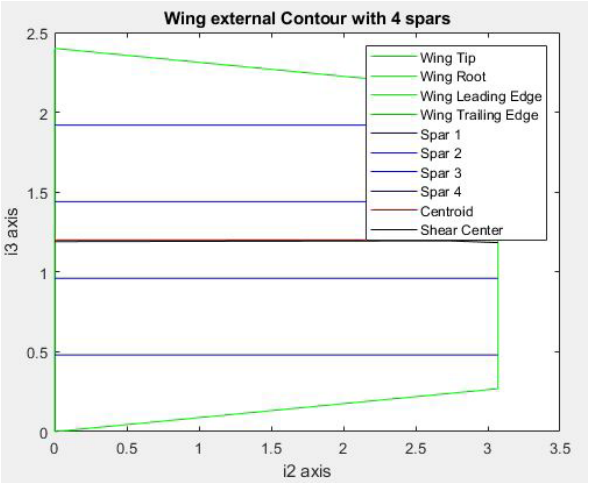

Fig. 15. Wing elastic and centroidal axis check

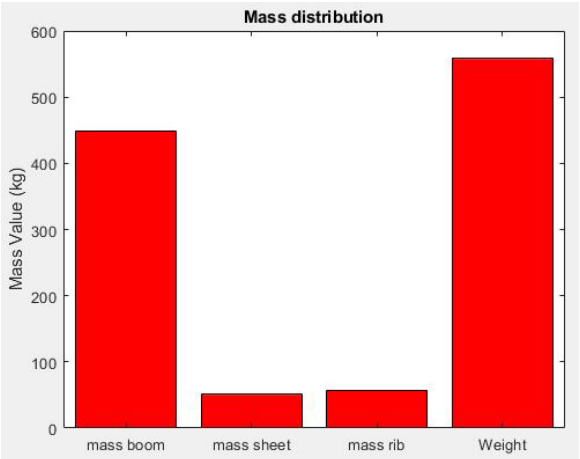

Fig. 16. Weight distribution of wing

5. Conclusion and recommendation

A case run for 2, and 3 spar cases was carried out, and values are displayed in Table 1. Comparative correlation of 2 spar and 3 spar models is done to understand the selection parameters.

Table 1. Comparison chart of case run of 2 and 3 spar

	2 spar model	3 spar model
Spar locations [m]	sp1 1 sp2 1.4	sp1 1 sp2 1.2 sp3 1.4
Centroid in i_2 at the root cross-section [m] (from trailing edge)	1.2	1.2
Shear centre in i_2 location at the root [m] (referred from centroid)	−0.00847	−0.01024
Bending stiffness at root [Nm^2]	1.54e7	1.474e7
Torsional stiffness at root [Nm^2]	3.01e6	3.008e6
Total mass [kg]	98.26	96.95
Boom mass contribution [kg]	82.92	82.92
Skin mass contribution [kg]	6.336	7.69
Ribs mass contribution [kg]	9.004	6.341

On the basis of results obtained in test case runs for different spar numbers and configuration, following user friendly functions of this code are identified:

- The Initial sizing of the wing requires automation to solve the differential equations. This can be done easily using MATLAB App Designer. This process simplifies the initial sizing of aircraft components and the validation of code.
- Input/output values can be displayed in multiple ways providing user freedom to use the most compatible tool for the required purpose.
- The optimization process requires a code that can be run for multiple iterations. This GUI provides a simple but effective optimization capability by selecting the variables bounds and constraints and defining any objective function.
- Sensitivity analysis of the input/output parameters can be done by carrying out the iteration multiple times with variations in the input value. GUI provides a powerful interface for this purpose.
- Standalone software extraction provides the user with the capability to distribute code or install it on several systems.

References

Bauchau, O.A., & Craig, J.I. (2009). *Structural Analysis* (1st ed.). Springer, Dordrecht.

Bruhn, E.F. (1973). *Analysis and Design of Flight Vehicle Structures* (2nd ed.). Tri-State Offset Company.

Dababneh, O., & Kayran, A. (2014). Design, analysis, and optimization of thin walled semi-monocoque wing structures using different structural idealization in the preliminary design phase. *International Journal of Structural Integrity*, *5*(3), 214–226. https://doi.org/10.1108/IJSI-12-2013-0050.

Giles, G.L. (1971). Procedure for automating aircraft wing structural design. *Journal of Structural Division*, *97*(1), 99–113.

Giles, G.L. (1986). Equivalent plate analysis of aircraft wing box structures with general planform geometry. *Journal of Aircraft*, *23*(11), 859–864.

Giles, G.L. (1994). Design-oriented structural analysis. In: B.H.V. Topping, M. Papadrakakis (Eds.), *Advances in Structural Engineering Computing* (pp. 1–10). Civil-Comp Press, https://www.doi.org/10.4203/ccp.29.1.1.

MathWorks (2018). *Documentation. MATLAB The Language of Technical Computing*, https://www.mathworks.com/help/matlab/.

Megson, T.H. (2017). *Aircraft Structures for Engineering Students* (6th ed.). Elsevier.

Niu, M.C.-Y. (2001). *Airframe Stress Analysis and Sizing* (2nd ed.). Adaso Adastra Engineering Center.

Niu, M.C.-Y. (2002). *Airframe Structural Design. Practical Design Information and Data on Aircraft Structures* (2nd ed.). Conmilit Press.

Raymer, D.P. (2018). *Aircraft Design. A Conceptual Approach* (6th ed.). American Institute of Aeronautics and Astronautics.

Youhua, L. (2000). *Efficient Methods for Structural Analysis of Built-Up Wings* [unpublished dissertation]. Virginia Polytechnic Institute and State University.

Youxu, Y., Wu, Z., & Yang, Ch. (2012). Equivalent plate modeling for complex wing configurations, *Procedia Engineering*, *31*, 409–415.